Original article

Resolution and Discovery 1 (2016) 1, pp. 2–8
DOI: 10.1556/2051.2016.00037

LORENTZ MICROSCOPY AND OFF-AXIS ELECTRON HOLOGRAPHY OF MAGNETIC SKYRMIONS IN FeGe

András Kovács[1*], Zi-An Li[2], Kiyou Shibata[3], Rafal E. Dunin-Borkowski[1]

[1]Ernst Ruska-Centre for Microscopy and Spectroscopy with Electrons and Peter Grünberg Institute, Forschungszentrum Jülich, D-52425 Jülich, Germany
[2]Faculty of Physics and Center for Nanointegration (CENIDE), University of Duisburg-Essen, D-48047 Duisburg, Germany
[3]RIKEN Center for Emergent Matter Science (CEMS), Wako 351-0198, Japan

Magnetic skyrmions are vortex-like spin structures that are of great interest scientifically and for applications in low-power magnetic memories. The nanometer size and complex spin structure require high-resolution and quantitative experimental methods to study the physical properties of skyrmions. Here, we illustrate how Lorentz TEM and off-axis electron holography can be used to study the spin textures of magnetic skyrmions in the noncentrosymmetric *B*20-type helimagnet FeGe as a function of temperature and applied magnetic field. By reversing the magnetic field inside the microscope, the switching mechanism of the skyrmion lattice at 240 K is followed, showing a transition of the skyrmion lattice to the helical structure before the anti-skyrmion lattice is formed.

Keywords: Lorentz microscopy, off-axis electron holography, magnetic skyrmions, FeGe

Introduction

Magnetic skyrmions are spin structures that have recently attracted considerable interest because of their topologically nontrivial physics and potential applications in energy-efficient spintronic devices for information technology [1]. In noncentrosymmetric *B*20-type helimagnets (e.g., MnSi, $Fe_{1-x}Co_xSi$ and $Mn_{1-x}Fe_xGe$) [2–5], broken inversion symmetry and relativistic spin-orbit coupling give rise to an asymmetric magnetic exchange interaction, which is termed the Dzyaloshinskii–Moriya interaction (DMI) [6, 7] and stabilizes the two- and three-dimensional localized structures of skyrmions. Recently, magnetic skyrmion structures have been observed in thin magnetic layers deposited on metallic substrates as a result of an interfacial DMI, which resulted in a magnetic ground state that was stable at room temperature in the absence of an external magnetic field [8, 9]. Skyrmions can form both Bloch- and Néel-type spin structures. In Bloch-type structures, the spins rotate in the plane parallel to the domain boundary, forming whirlpool-like textures that have been observed in chiral magnets [2–5]. In contrast, the spins in Néel-type skyrmions rotate in the radial plane from the core to the periphery, i.e., in a plane perpendicular to the domain boundary [10]. Magnetic skyrmion formation was first confirmed experimentally in MnSi using small angle neutron scattering in momentum space [2]. Subsequently, a skyrmion lattice was observed in $Fe_{0.5}Co_{0.5}Si$ using Lorentz transmission electron microscopy (LTEM) [3] in real space. Since then, LTEM and related techniques have been used extensively to study skyrmions. Examples include studies of the formation and fluctuation of skyrmion domains in Cu_2OSeO_3 [11], the anisotropic deformation of skyrmions in a strained crystal [12], and reports of the formation and collective dynamics of a skyrmion chain in a confined geometry [13].

LTEM involves the acquisition of defocused Fresnel images of a specimen and relies on the deflection of electrons by magnetic fields within and around the sample. However, the quantitative interpretation of Fresnel images of skyrmions can be difficult, primarily because strong additional contributions to the contrast can result from local variations in specimen thickness and composition and because the analysis of recorded images using approaches based on the transport of intensity equation (TIE) can introduce artefacts resulting from noise and unknown boundary conditions. In contrast, the TEM mode of off-axis electron holography allows the phase shift of the electron wave that has passed through an electron-transparent specimen to be recorded directly with nanometre spatial resolution. Unwanted contributions to the phase, such as those associated with local changes in specimen thickness and composition, can be removed from recorded phase images much more easily than from images recorded using either LTEM or other techniques such as differential contrast imaging in the scanning TEM. Park et al. [14] have previously used off-axis electron holography to study the three-dimensional magnetic structure of skyrmions in *B*20-type $Fe_{0.5}Co_{0.5}Si$.

* Corresponding author: András Kovács; E-mail: a.kovacs@fz-juelich.de

First published online: October 24, 2016

Here, we illustrate the dependence on magnetic field and temperature of skyrmion evolution in a *B*20-type FeGe single crystal using both LTEM and electron holography. In bulk form, FeGe is known to exhibit a near-room-temperature helical transformation (at 278 K) and to have a low value of magnetocrystalline anisotropy. We outline the methods of magnetic imaging of skyrmions in a TEM and procedures for extracting magnetic induction maps. We also study the magnetization reversal process of a skyrmion lattice under control of the external field using *in situ* LTEM.

Experimental details

TEM specimens were prepared from a single crystal of *B*20-type FeGe using a focused ion beam (FIB) workstation and a lift-out method to have a uniform thickness of ~100 nm and a large lateral dimension of ~50 μm^2. FIB-induced damage was removed by using low energy (900 eV) Ar ion milling in a Fischione Nanomill system. LTEM (Fresnel defocus) images and off-axis electron holograms were recorded at 300 kV using an FEI Titan 60–300 TEM. The microscope was operated in magnetic-field-free conditions (<0.5 mT) in aberration-corrected Lorentz mode and is equipped with a Gatan Ultrascan 2k × 2k charge-coupled device (CCD) camera and an electrostatic biprism [15]. The conventional microscope objective lens could be used to apply chosen vertical (out-of-plane) magnetic fields of between 0 and 1.5 T, which were precalibrated using a Hall probe. In addition, the ability to reverse the direction of the magnetic field of the objective lens allowed magnetization reversal of the skyrmion lattice to be studied. A liquid nitrogen specimen holder (Gatan model 636) was used to vary the specimen temperature between 95 and 370 K. Real-space phase images were reconstructed from recorded off-axis electron holograms using scripts written in the Semper image processing language [16].

Results and discussion

LTEM and transport of intensity equation analysis

A key requirement for studying magnetic materials in the TEM is to place the sample in a magnetic-field-free environment. This situation is usually achieved by turning off the conventional microscope objective lens and using, instead, either a dedicated Lorentz mini-lens or the transfer lens of the objective lens aberration corrector. As both lenses are located far from the sample, the electron-optical performance of the microscope is then decreased. A spherical aberration corrector can be used to reduce the spherical aberration coefficient (C_s) of the Lorentz lens from several metres to below 1 mm, in order to provide improved spatial resolution, as shown schematically in *Figure 1*(*a*).

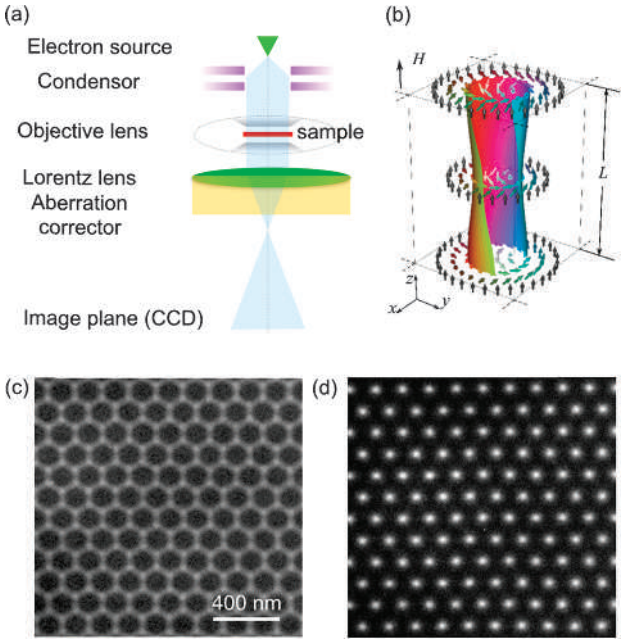

Fig. 1. (a) Schematic representation of the electron-optical elements used in Lorentz TEM. The objective lens is turned off to produce a magnetic-field-free condition at the position of the sample. (b) Magnetic configuration of a Bloch-type skyrmion in a thin film of thickness *L* and in the presence of *H* magnetic field. (c) Underfocus and (d) overfocus Fresnel images of a skyrmion lattice in an FeGe specimen formed in the presence of a 100 mT applied magnetic field at a temperature of 200 K. The images were recorded at defocus values of ±0.4 mm

In LTEM, incident electrons are deflected by the Lorentz force:

$$F_{\mathrm{L}} = -e(E + v \times B),$$

as a result of the presence of an electrostatic field E and/or a magnetic field B within and around the sample. In LTEM, only the in-plane components of the magnetic induction B_{xy} contribute to the deflection angle, which is typically in the range of a few tenths of a μrad, i.e., much smaller than a typical Bragg angle of a few milliradians. Large defocus values are often needed to generate appreciable magnetic contrast.

Figure 1(*b*) shows the magnetic configuration of a single skyrmion in a thin film with a Bloch-type spin texture. The magnetization directions in the middle and at the edges of the skyrmion are antiparallel to each other. When traversing such skyrmions, incident electrons will either diverge or converge, resulting in circles of contrast in defocused Fresnel images, with the sense of the contrast depending on the helicity of the spins and on the defocus value used, as shown in *Figure 1*(*c*) and (*d*). Such imaging conditions have been used to determine the magnetic helicities of skyrmions and their dependence on crystal chirality [5, 17].

The TIE which was originally proposed by Teague [18], is a phase retrieval method that relies on the relationship between the intensity derivative in the electron beam direction (measured from images recorded at

different defocus values) and the lateral phase variation. Subsequent modification and enhancement of the technique have enabled quantitative phase measurement in some cases. Successful examples include recent applications to imaging magnetic skyrmions. Here, we implemented a Fourier-transform-based TIE approach [19] with a Tikhonov-type low frequency filter in a custom-designed Matlab code and analyzed the resulting TIE-derived phase images. *Figures 2*(*a*–*c*) show Fresnel defocus images of a skyrmion lattice in FeGe, to which TIE analysis was applied to yield a phase image. Since this specimen is flat, the electrostatic (mean inner potential) contribution the phase can be assumed to be constant and the resulting phase variation can be considered to be magnetic in origin. On this assumption, a color map, in which the hue represents the direction of the projected in-plane magnetic induction, was created from the gradients of the TIE-derived magnetic phase, as shown in *Figure 2*(*d*). Although separation of the electrostatic and magnetic contributions to a TIE-derived phase image is in principle possible, care is required to avoid introducing artefacts [20].

The design of the objective lens in the FEI Titan microscope used in the present study allowed magnetization reversal of skyrmions to be studied *in situ*, as shown in *Figure 3*. The LTEM images show that the starting state was a perfect lattice of skyrmions, which formed in a 100 mT out-of-plane magnetic field at 240 K. The magnetic field was decreased gradually by changing the objective lens excitation using the microscope's free lens control. At a magnetic field of +65 mT, the skyrmion lattice was partially destroyed and a local helical structure emerged at the expense of the skyrmions. As the strength of the magnetic field was increased in the opposite direction, the helical structure transformed into a skyrmion lattice at a field of −95 mT. The reverse process went through the same steps, with the anti-skyrmion lattice transforming to the helical structure and then to the original skyrmion lattice in a quick transition. The results show that the magnetization reversal process that occurs when the magnetic field direction is reversed involves a transition through a helical structure before an anti-skyrmion lattice forms at a given substrate temperature.

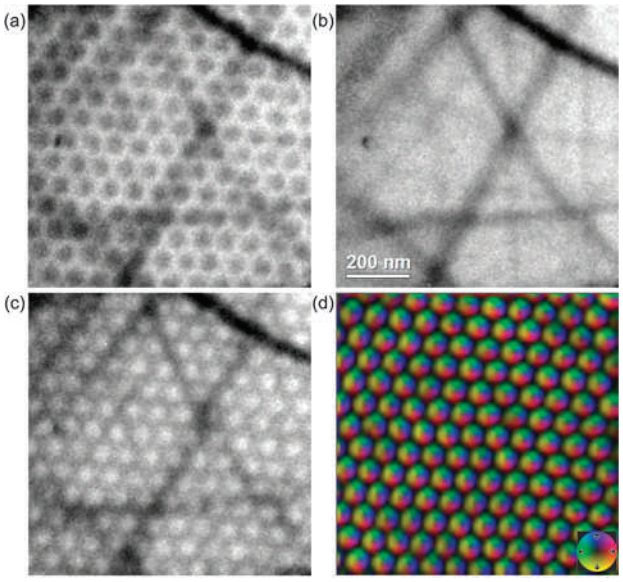

Fig. 2. Transport of intensity equation analysis of a magnetic skyrmion lattice in FeGe recorded at 220 K in the presence of 100 mT magnetic field. (a–c) Fresnel defocus images recorded at defocus values of −200, 0, and +200 μm, respectively. (d) Magnetic induction map generated from the gradients of the phase distribution recovered from images (a–c) using the transport of intensity equation

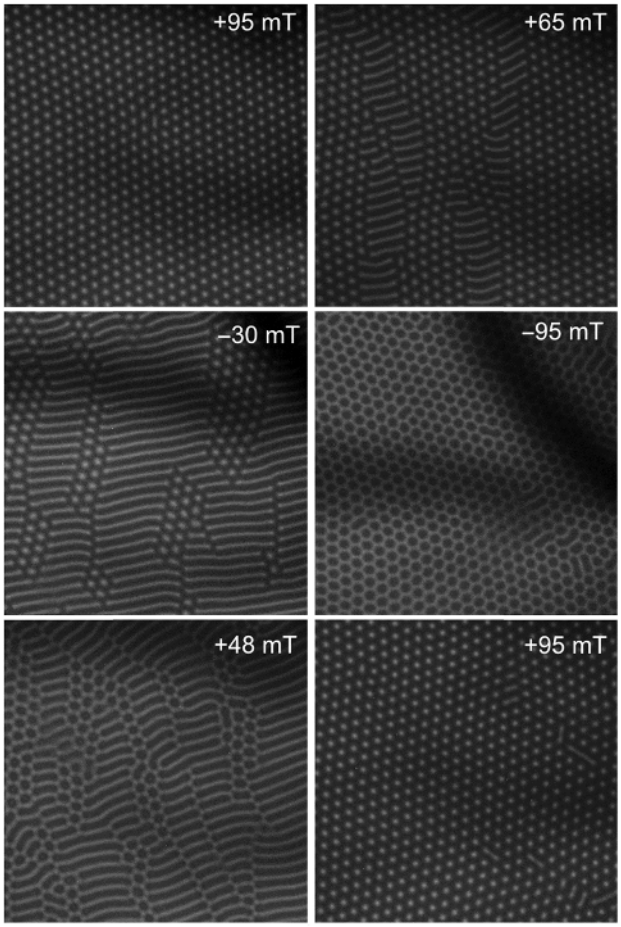

Fig. 3. Overfocus Fresnel images (defocus ~1 mm) recorded at specimen temperature of 240 K, demonstrating *in situ* switching of skyrmion polarity by applying the indicated magnetic fields to the sample using the objective lens of the TEM

Quantitative magnetic induction mapping of skyrmions

Off-axis electron holography is based on the interference of electron waves that have passed through the sample (object wave) and vacuum (reference wave), as shown schematically in *Figure 4*(*a*). Holographic interference fringes are typically generated by applying a positive voltage to a biprism wire positioned close to one of the conjugate image planes in the microscope. The interference fringe spacing and the width of the overlap region are controlled by the biprism voltage and the microscope lens setup. Most

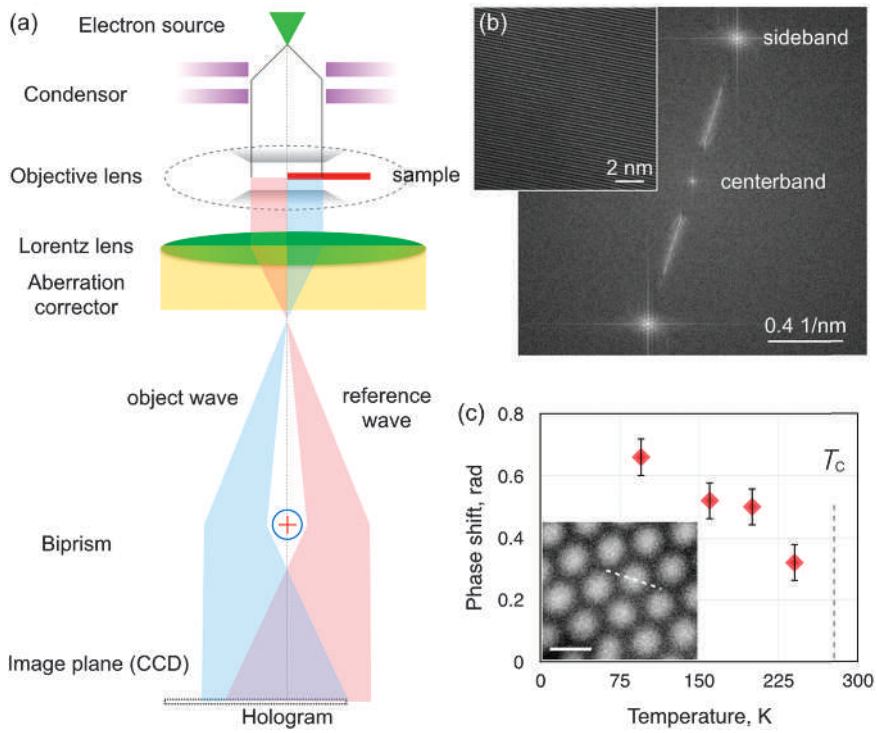

Fig. 4. (a) Schematic diagram showing the setup for off-axis electron holography. (b) Off-axis electron hologram of a skyrmion lattice in FeGe and the Fourier transform of the hologram. The streak between the centerband and the sideband is associated with Fresnel fringes at the edges of the biprism wire. (c) Magnetic phase shift of skyrmions measured as a function of temperature. The inset shows a phase image of the skyrmion lattice. Dashed line marks the line-scan region used to measure the phase shift. The scale bar is 90 nm

commonly, a single biprism is used in the selected area aperture position, while the electron-optical configuration is chosen by changing the excitation of the diffraction or intermediate lenses. However, there are also many other variations of electron holography [21–24]. *Figure 4*(*b*) shows part of an off-axis electron hologram recorded at 200 K in the presence of a 100 mT magnetic field. The inset shows a Fourier transform of the hologram. The streak between the centerband and the sidebands is attributed to Fresnel fringes from the edges of the biprism wire. Inverse Fourier transformation of one of the sidebands is used to recover the complex wave function, which can be displayed in the form of amplitude and phase images [25]. When digital processing is used to perform reconstruction of electron holograms, the resulting phase images are normally calculated modulo 2π. Phase unwrapping algorithms can then be used to remove phase discontinuities.

Neglecting dynamical diffraction, the measured phase shift can be expressed in the form:

$$\phi(x) = C_{\mathrm{E}} \int V(x,z)dz - \left(\frac{e}{\hbar}\right) \iint B(x,z)dxdz$$

where z is the incident electron beam direction, x is a direction in the plane of the sample, C_{E} is a constant that depends on the microscope accelerating voltage, V is the electrostatic potential, and B is the in-plane component of the magnetic induction. If neither V nor B varies in the incident electron beam direction, then the above equation can be simplified to:

$$\phi(x) = C_{\mathrm{E}} V(x)t(x) - \left(\frac{e}{\hbar}\right) \int B(x)t(x)dx,$$

where t is the sample thickness. Further differentiation and removal of the electrostatic contribution to the phase result in an expression for the phase gradient, which is directly proportional to the in-plane component of the in-plane magnetic induction:

$$\frac{d\phi(x)}{dx} = \left(\frac{et(x)}{\hbar}\right) B(x).$$

In order to measure the magnetic phase shift associated with skyrmions, pairs of off-axis electron holograms were recorded and subtracted from each other. One of the holograms was measured at the sample temperature of interest (below the Curie temperature of 278 K), while the other hologram was measured at room temperature (above the Curie temperature), in order to ensure the absence of magnetic contrast. This approach relies on the electrostatic contribution to the phase being unchanged between the two temperatures. *Figure 4*(*c*) shows the magnetic phase of skyrmions measured using this approach as a function of temperature. The magnetic phase shift decreases, and the skyrmions disappear as the

temperature approaches 278 K, confirming that the critical or Curie temperature for skyrmions in a thin film is the same as that in bulk FeGe.

Figure 5 shows the strength and direction of the local projected in-plane magnetic induction in the FeGe sample displayed in the form of phase contours and colors. The initial helical structure is associated with an in-plane rotation of the magnetization and has a periodicity of approximately 70 nm. The application of a magnetic field normal to the sample plane results in a gradual transformation of the helices into skyrmions. *Figure 5*(*b*) and (*c*) show corresponding color-contour maps of the skyrmions measured at 95 and 240 K, respectively. The magnetic phase contours have a spacing of $2\pi/64$ radians, corresponding to an enclosed magnetic flux between any two contours of $4\pi/64 \times 10^{-15}$ Wb. The handedness of the skyrmions stays the same at the different applied magnetic fields, but the density of the magnetic phase contour lines decreases as the temperature approaches the Curie temperature of the sample. The phase maps also reveal that the skyrmions move slightly and form dislocations. However, the three-fold symmetry of the skyrmion lattice remains stable at the higher temperature.

The magnetic field dependence of the skyrmion lattice was studied by applying a perpendicular magnetic field to the sample using the objective lens of the microscope. *Figure 6* shows transformations of the skyrmion lattice as the magnetic field was increased to 400 mT at a constant sample temperature of 200 K. As the magnetic field was increased to 300 mT, the skyrmion lattice started to deviate from a triangular lattice, becoming disordered at approximately 350 mT. A gradual decrease in the skyrmion core was accompanied by an expansion of the lattice period. At 400 mT, the number of skyrmions decreased significantly. Between adjacent skyrmions, the sample was then saturated magnetically perpendicular to its surface. At 450 mT, the skyrmions disappeared and the sample was fully saturated magnetically parallel to the applied field direction. The measured magnetic phase shifts of individual skyrmions were observed to decrease with increasing applied field, as shown in *Figure 6*(*e*).

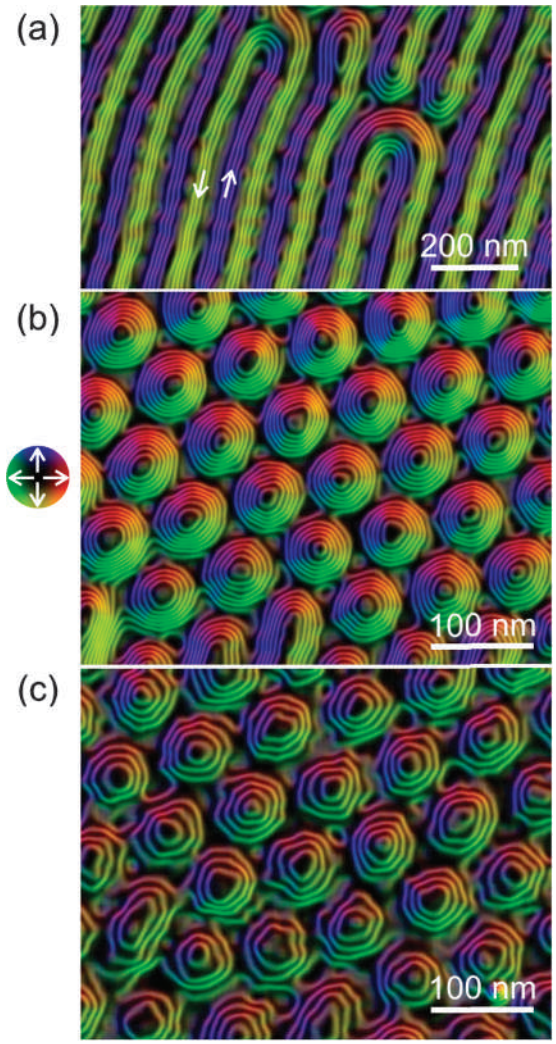

Fig. 5. Magnetic induction maps determined from magnetic phase images recorded using off-axis electron holography, corresponding to (a) a ground state helical structure in zero applied field and to skyrmion lattices measured at (b) 95 and (c) 240 K in an out-of-plane magnetic field of 100 mT. The magnetic phase contour spacing is $2\pi/64 = 0.098$ radians

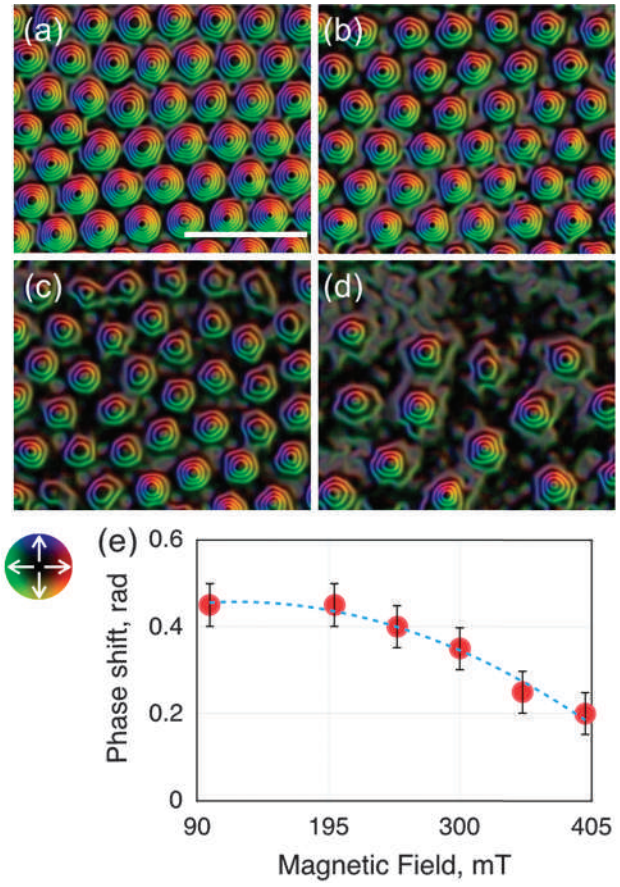

Fig. 6. Magnetic induction maps recorded using off-axis electron holography showing the magnetic field dependence of a skyrmion lattice at 200 K, shown for applied magnetic fields of (a) 200, (b) 300, (c) 350, and (d) 400 mT. The magnetic phase contour spacing is $2\pi/64 = 0.098$ radians. The scale bar is 200 nm. (e) Magnetic phase shift of individual skyrmions measured at different magnetic fields

By calculating the spin rotation angle of the skyrmions from the phase images as a function of temperature and magnetic field [26], it was found that the skyrmion structure shows no significant dependence on sample temperature, while it shows a modulation with increasing magnetic field [27]. Based on the magnetic profiles of the skyrmions, a phenomenological model was developed to describe the change in the in-plane profile of the skyrmions as a function of magnetic field [26].

Summary

Lorentz TEM and off-axis electron holography have been used to perform high spatial resolution magnetic imaging of helical states and Bloch-type magnetic skyrmions in FeGe as a function of sample temperatures and applied magnetic field. By reversing the magnetic field *in situ* inside the microscope, the magnetization switching mechanism of the skyrmion lattice was monitored at 240 K, showing a transition through a helical structure before an anti-skyrmion lattice formed. The temperature dependence of the skyrmion lattice was studied between 95 K and 260 K, confirming that the Curie temperature in a thin film is the same as that in bulk FeGe. The magnetic field dependence of the skyrmion lattice showed disorder and a decrease in the magnetization as the field increased. Beyond the high-resolution and quantitative observation of magnetic skyrmions presented in this work, the application of electrical biasing and in-plane magnetic fields can be used in future TEM studies.

Acknowledgement

The authors would like to thank to N. Kiselev, S. Blügel, N. Kanazawa, and Y. Tokura for their support and valuable discussions. The research leading to these results received funding from the European Research Council under the European Union's Seventh Framework Programme (FP7/2007-2013)/ERC grant agreement number 320832.

References

1. Kiselev NS, Bogdanov AN, Schäfer R, Rössler UK: Chiral skyrmions in thin magnetic films: new objects for magnetic storage technologies? J Phys D Appl Phys 44, 392001 (2011)
2. Mühlbauer S, Binz B, Jonietz F, Pfleiderer C, Rosch A, Neubauer A, Georgii R, Böni P: Skyrmion lattice in a chiral magnet. Science 323, 915 (2009)
3. Yu XZ, Onose Y, Kanazawa N, Park JH, Han JH, Matsui Y, Nagaosa N, Tokura Y: Real-space observation of a two-dimensional skyrmion crystal. Nature 465, 901 (2010)
4. Yu XZ, Kanazawa N, Onose Y, Kimoto K, Zhang WZ, Ishiiwata S, Matsui Y, Tokura Y: Near room temperature formation of a skyrmion crystal in thin-films of the helimagnet FeGe. Nat Mater 10, 106 (2011)
5. Shibata K, Yu XZ, Morikawa D, Kanazawa N, Kimoto K, Ishiwata S, Matsui Y, Tokura Y: Towards control of the size and helicity of skyrmions in helimagnetic alloys by spin-orbit coupling. Nat Nanotechnol 8, 723 (2013)
6. Dzyaloshinsky I: Thermodynamic theory of weak ferromagnetism in antiferromagnetic substances. J Phys Chem Solids 4, 241 (1958)
7. Moriya T: Anisotropic superexchange interaction and weak ferromagnetism. Phys Rev 120, 91 (1960)
8. Heinze S, von Bergmann K, Menzel M, Brede J, Kubetzka A, Wiesendanger R, Bihlmayer G, Blügel S: Spontaneous atomic-scale magnetic skyrmion lattice in two dimensions. Nat Phys 7, 713 (2011)
9. Woo S, Litzius K, Krüger B, Im MY, Caretta L, Richter K, Mann M, Krone A, Reeve RM, Weigand M, Agrawal P, Lemesh I, Mawass MA, Fischer P, Kläui M, Beach GSD: Observation of room-temperature magnetic skyrmions and their current-driven dynamics in ultrathin metallic ferromagnets. Nat Mater 15, 501 (2016)
10. Kézsmárki I, Bordács S, Milde P, Neuber E, Eng LM, White JS, Rønnow HM, Dewhurst CD, Mochizuki M, Yanai K, Nakamura H, Ehlers D, Tsurkan V, Loidl A: Néel-type skyrmion lattice with confined orientation in the polar magnetic semiconductor GaV_4S_8. Nat Mater 14, 1116 (2015)
11. Rajeswari J, Huang P, Mancini GF, Murooka Y, Latychevskaia T, McGrouther D, Cantoni M, Baldini E, White JS, Magrez A, Giamarchi T, Rønnow HM, Carbone F: Filming the formation and fluctuation of skyrmion domains by cryo-Lorentz transmission electron microscopy. Proc Natl Acad Sci 112, 14212 (2015)
12. Shibata K, Iwasaki J, Kanazawa N, Aizawa S, Tanigaki T, Shirai M, Nakajima T, Kubota M, Kawasaki M, Park HS, Shindo D, Nagaosa N, Tokura Y: Large anisotropic deformation of skyrmions in strained crystal. Nat Nanotechnol 10, 589 (2015)
13. Du H, Che R, Kong L, Zhao X, Jin C, Wang C, Yang J, Ning W, Li R, Jin C, Chen X, Zang J, Zhang Y, Tian M: Edge mediated skyrmion chain and its collective dynamics in a confined geometry. Nat Commun 6, 8504 (2015)
14. Park HS, Yu X, Aizawa S, Tanigaki T, Akashi T, Takahashi Y, Matsuda T, Kanazawa N, Onose Y, Shindo D, Tonomura A, Tokura Y: Observation of the magnetic flux and three-dimensional structure of skyrmion lattices by electron holography. Nat Nanotechnol 9, 337 (2014)
15. Boothroyd C, Kovács A, Tillmann K: FEI Titan G2 60-300 HOLO. J Large-Scale Facil 2, A44 (2016)
16. Saxton WO, Pitt TJ, Horner M: Digital image processing: the Semper system. Ultramicroscopy 4, 343 (1979)
17. Morikawa D, Shibata K, Kanazawa N, Yu XZ, Tokura Y: Phys Rev B 88, 024408 (2013)
18. Tegue MR: Deterministic phase retrieval: a Green's function solution. J Opt Soc Am 73, 1434 (1983)
19. Ishizuka K, Allman B: Phase measurement of atomic resolution imaging using transport of intensity equation. J Electron Microsc 54, 191 (2005)
20. Phatak C, Petford-Long AK, De Graef M: Recent advances in Lorentz microscopy. Curr Opin Solid State Mater Sci 20, 107 (2016)
21. Cowley JM: Twenty forms of electron holography. Ultramicroscopy 41, 335 (1992)
22. Tanigaki T, Harada K, Murakami Y, Niitsu K, Akashi T, Takahashi Y, Sugawara A, Shindo D: New trend in electron holography. J Phys D Appl Phys 49, 244001 (2016)

23. McCartney MR, Smith DJ: Electron holography: phase imaging with nanometer resolution. Annu Rev Mater Res 37, 729 (2007)
24. Lichte H, Lehmann M: Electron holography — basics and applications. Rep Prog Phys 71, 016102 (2008)
25. Dunin-Borkowski RE, McCartney MR, Smith DJ: Electron holography of nanostructured materials. Encycl Nanosci Nanotechnol 3, 41 (2004)
26. Shibata K, Kovács A, Kanazawa N, Dunin-Borkowski RE, Tokura Y: Temperature and magnetic field dependence of the internal and lattice structures of skyrmions by off-axis electron holography. submitted, arXiv:1606.05723
27. Rybakov FN, Borisov AB, Bogdanov AN: Three-dimensional skyrmion states in thin films of cubic helimagnets. Phys Rev B 87, 094424 (2013)